Spring 6-6-2018

Formazanate Complexes of Hypervalent Group-14 Elements as Precursors to Electronically Stabilized Radicals

Ryan R. Maar

Sara D. Catingan

Viktor N. Staroverov

Joe Gilroy
jgilroy5@uwo.ca

Formazanate Complexes of Hypervalent Group-14 Elements as Precursors to Electronically Stabilized Radicals

Ryan R. Maar,[a] Sara D. Catingan,[a] Viktor N. Staroverov,[a] and Joe B. Gilroy*[a]

Abstract: The stability of molecular radicals containing main-group elements usually hinges on the presence of bulky substituents that shield the reactive radical center. We describe a family of group-14 formazanate complexes whose chemical reduction allows access to radicals that are stabilized instead by geometric and electron-delocalization effects, specifically by the square-pyramidal coordination geometry adopted by the group-14 atom (Si, Ge, Sn) within the framework of the heteroatom-rich formazanate ligands. The reduction potentials of the Si, Ge, and Sn complexes as determined by cyclic voltammetry become more negative in that order. Examination of the solid-state structures of these complexes suggested that their electron-accepting ability decreases with increasing group-14 atom size because a larger central atom increases the nonplanarity of the ligand-based conjugated π-electron system of the complex. The experimental findings were supported by density-functional calculations on the parent complexes and the corresponding radical anions.

The ability to synthesize, isolate, and characterize molecular compounds that defy conventional chemical bonding models is a long-standing goal of the main-group chemistry community. In this context, open-shell systems (*i.e.*, radicals) of main-group compounds have received significant attention.[1] In particular, stable radicals[2] containing group-14 elements (E = Si, Ge, or Sn)[3] have been structurally characterized by the Power[4] (**1**) and Sekiguchi (**2**[5] and **3**[6]) groups. The key to isolating these reactive species is the stabilization afforded by the large aromatic and persilyl substituents present in the supporting ligand backbones.[7] Another effective way to stabilize group-14 radicals is to combine bulky substituents with strongly σ-donating ligands. To that end, *N*-heterocyclic carbenes,[8] and cyclic alkyl(amino) carbenes[9] are most frequently used. The outcome is exemplified by compound **4**, which is comprised of a sterically-imposing carbene that acts both as a σ-donor and π-acceptor to stabilize the unpaired electron.[10] A third approach involves the combination of bulky substituents and chelating ligands such as β-diketiminates,[11] which have the potential to stabilize the radical through inductive effects and electron delocalization. In that manner, the Jones and co-workers isolated compound **5**, the first example of a neutral, monomeric Ge(I)-centered radical.[12] More recently, Wang *et al.*[13] demonstrated that structural modification of the β-diketiminate backbone leads to the formation of complex **6**, a ligand-centered radical.

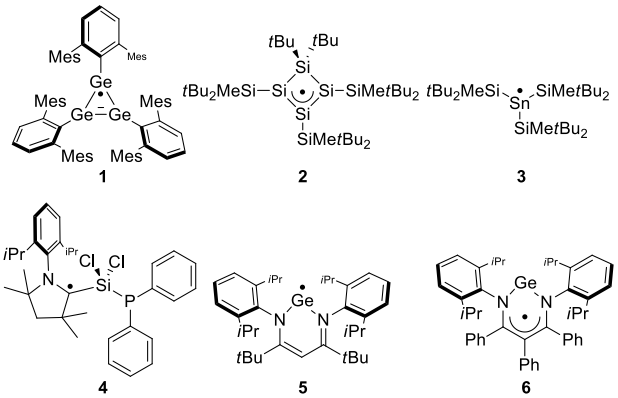

Here, we report complexes and radicals containing hypervalent group-14 elements supported by a tetradentate $N_2O_2^{3-}$ formazanate ligand.[14] These radicals do not benefit from appreciable steric bulk and appear to be stabilized via extended electron delocalization over multiple electronegative atoms. The quasi-square-pyramidal geometry adopted by the group-14 elements in such complexes plays a critical role in this process.

The target complexes **8–10** were prepared according to Scheme 1 (Figures S1–S6). Formazan **7**[15] was treated with excess NaH to generate the corresponding trianion, which was then reacted with the appropriate group-14-containing phenyltrichloride ($EPhCl_3$; E = Si, Ge, or Sn) to give complexes **8–10** in 53–65% yield. Radicals $\mathbf{8}^{\bullet-}$–$\mathbf{10}^{\bullet-}$ were prepared by reacting the parent formazanate complex with bis(pentamethylcyclopentadienyl)cobalt ($CoCp^*_2$) and isolated in 62% ($\mathbf{8}^{\bullet-}$) and 61% ($\mathbf{9}^{\bullet-}$) yield (see the Supporting Information for details). While radicals $\mathbf{8}^{\bullet-}$ and $\mathbf{9}^{\bullet-}$ could be isolated and structurally characterized, the Sn analog $\mathbf{10}^{\bullet-}$ proved to be unstable (see below).

Complexes **8–10** absorbed throughout the visible region of the electromagnetic spectrum and particularly strongly at longer wavelengths (Figures 1a–c). Complex **8** had absorption maxima (λ_{max}) at 662 nm (ε = 16,800 M^{-1} cm^{-1}), 474 nm (ε = 3,700 M^{-1} cm^{-1}), and 329 nm (ε = 14,600 M^{-1} cm^{-1}). The spectra of complexes **9** [λ_{max}: 681 nm (ε = 21,200 M^{-1} cm^{-1}); 472 nm (ε = 4,400 M^{-1} cm^{-1}); 331 nm (ε = 18,500 M^{-1} cm^{-1})] and **10** [λ_{max}: 681 nm (ε = 22,200 M^{-1} cm^{-1}); 463 nm (ε = 4,600 M^{-1} cm^{-1}); 333 nm (ε = 17,000 M^{-1} cm^{-1})] were similar. The experimental UV-vis absorption spectra were qualitatively reproduced by adiabatic linear-response time-dependent density functional theory calculations performed with the *Gaussian* program[16] using the PBE1PBE functional,[17] 6-311+G* basis set, and implicit solvation methods (Figure S7 and Table S3). The calculations showed that the observed lowest-energy electronic transitions have π→π* character and involve highly delocalized molecular orbitals (Figures 2a, S8, and S9).

[a] R. R. Maar, S. D. Catingan, Prof. Dr. V. N. Staroverov, Prof. Dr. J. B. Gilroy
Department of Chemistry and The Centre for Advanced Materials and Biomaterials Research (CAMBR)
The University of Western Ontario
1151 Richmond St. N., London, Ontario N6A 5B7, Canada.
E-mail: joe.gilroy@uwo.ca

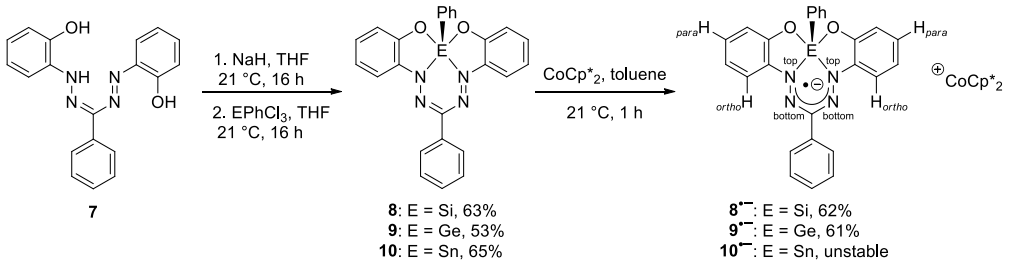

Scheme 1. Synthetic route to group-14 formazanates **8**–**10** and radical anions **8**$^{\bullet-}$–**10**$^{\bullet-}$.

Chemical reduction of **8**–**10** was accompanied by three major changes to the corresponding absorption spectra: 1) the disappearance of the lowest-energy absorption band, 2) the appearance of a broad absorption band red-shifted relative to the parent complexes [**8**$^{\bullet-}$: λ_{max} = 772 nm (ε = 3,300 M^{-1} cm^{-1}); **9**$^{\bullet-}$: λ_{max} = 813 nm (ε = 4,600 M^{-1} cm^{-1})], and 3) the appearance of a peak blue-shifted relative to the parent complexes [**8**$^{\bullet-}$: λ_{max} = 483 nm (ε = 5,000 M^{-1} cm^{-1}); **9**$^{\bullet-}$: λ_{max} = 485 nm (ε = 7,800 M^{-1} cm^{-1})] (Figures 1a–c). These observations suggest the formation of a formazanate-centered radical.[18]

Electron paramagnetic resonance (EPR) spectra, collected for dry, degassed CH_2Cl_2 solutions of **8**$^{\bullet-}$ (*g* = 2.0037) and **9**$^{\bullet-}$ (*g* = 2.0035) were well-resolved (Figures 1d and 1e). The isotropic hyperfine coupling constants (*a*) for the N and H atoms labelled in Scheme 1 were extracted from these spectra using the EasySpin software package[19] and were found to be as follows: **8**$^{\bullet-}$: $a_{N(bottom)}$ = 5.05 G, $a_{N(top)}$ = 3.37 G, $a_{H(ortho)}$ = 1.61 G, $a_{H(para)}$ = 1.58 G; **9**$^{\bullet-}$: $a_{N(bottom)}$ = 4.94 G, $a_{N(top)}$ = 3.75 G, $a_{H(ortho)}$ = 1.56 G, $a_{H(para)}$ = 1.55 G. All of these constants were consistent with the theoretically predicted values (Table S4). The calculated singly-occupied molecular orbitals (SOMOs) and spin-density maps of **8**$^{\bullet-}$ and **9**$^{\bullet-}$ (Figures 2a and S8) indicate that the unpaired electron is most likely to be found on the formazante nitrogen atoms. Note that the low relative abundance of the spin-active isotopes of Si and Ge did not allow us to extract the experimental hyperfine constants for these atoms; the density-functional calculations predicted a_{Si} = 4.0 G and a_{Ge} = 2.3 G (Tables S5 and S6).

To understand the difficulties encountered during the attempted isolation of radical **10**$^{\bullet-}$ (E = Sn), we probed the electron-accepting abilities of complexes **8**–**10** using cyclic voltammetry (CV) (Figure 1f). The CV data showed that compounds **8** and **9** undergo two one-electron, reversible electrochemical reductions (**8**: E_{red1} = –0.91 V, E_{red2} = –1.84 V; **9**: E_{red1} = –0.98 V, E_{red2} = –1.86 V relative to the ferrocene/ferrocenium redox couple), which correspond to the formation of a radical anions and dianions, respectively. In contrast, complex **10** exhibited two irreversible one-electron reductions at –1.10 V and –1.88 V. The more negative reduction potentials observed for complex **10** and the lack of reversibility of the reduction events in the CV are consistent with the generation of highly reactive species. They also provide evidence that complex **10** is a poorer electron-acceptor compared to complexes **8** and **9**.

Examination of the experimental solid-state structures and the calculated gas-phase geometries of complexes **8**–**10** and

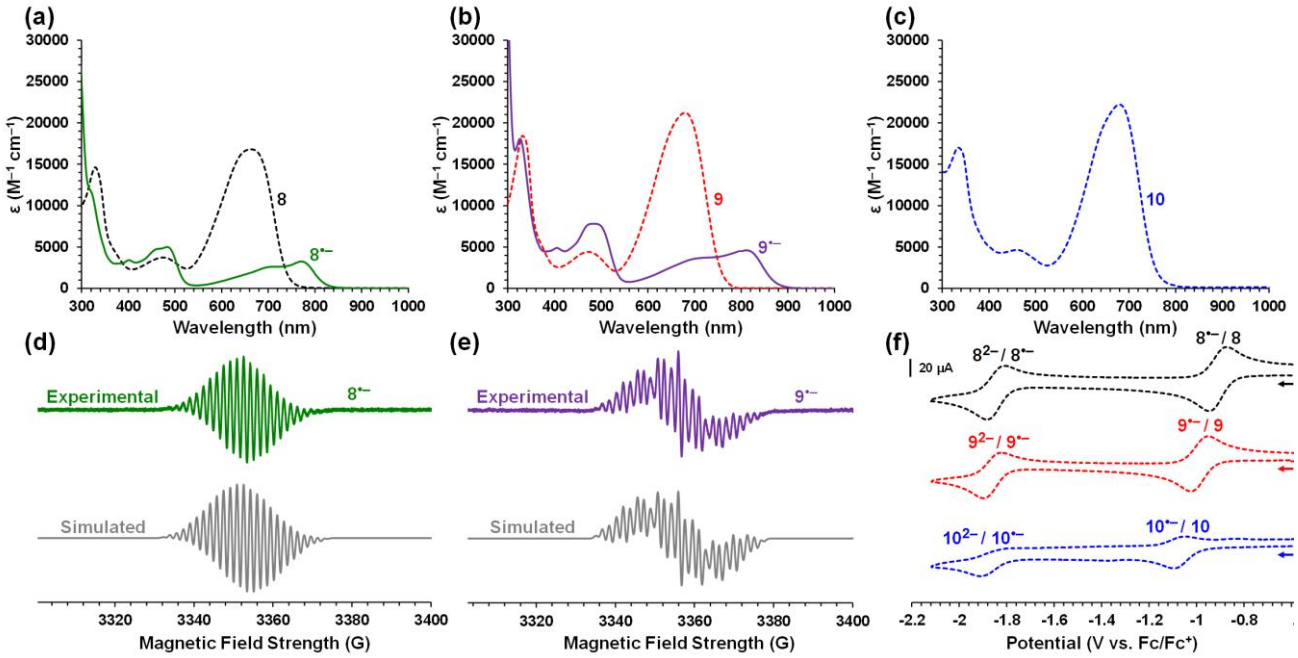

Figure 1. (a–c) UV-vis absorption spectra of complexes **8**–**10** and radicals **8**$^{\bullet-}$ and **9**$^{\bullet-}$ recorded for 20 μM dry, degassed CH_2Cl_2 solutions. (d, e) EPR spectra of radicals **8**$^{\bullet-}$ and **9**$^{\bullet-}$ recorded for 40 μM (**8**$^{\bullet-}$) and 60 μM (**9**$^{\bullet-}$) dry, degassed CH_2Cl_2 solutions at 21 °C. (f) Cyclic voltammograms of complexes **8**–**10** recorded in dry, degassed CH_2Cl_2 containing ~1 mM analyte and 0.1 M [$n$$Bu_4N$][$PF_6$] at a scan rate of 250 mV s^{-1}. The arrows denote the scan direction.

radicals **8**$^{\bullet-}$ and **9**$^{\bullet-}$ (Figures 2b, S8, S9, Tables S1 and S2) revealed that these molecules adopt an approximately square-pyramidal geometry at the group-14 atoms, which is in stark contrast with the trigonal-bipyramidal geometry reported by Nabeshima *et al.*[20] for structurally-related group-14 N_2O_2 dipyrrinate complexes, likely due to differences between the five-membered (formazanate) and six-membered (dipyrrinate) chelate rings. This observation was quantified by computing the structural parameter τ of Addison and co-workers, which is defined in such a way that it has a value of 0 for a perfect square-pyramidal geometry and a value of 1 for an ideal trigonal bipyramid.[21] Complexes **8**–**10** and radicals **8**$^{\bullet-}$ and **9**$^{\bullet-}$ have τ values between 0.02 and 0.15 compared to τ = 0.82, 0.67, and 0.59 for the analogous group-14 N_2O_2 dipyrrinates.

The size of the group-14 atom has a significant effect on the relative co-planarity of the N_2O_2 binding pocket and ligand backbone. Specifically, the larger O2-E-O1 bond angle (θ_1) of complex **10** [94.58(18)°] relative to complexes **9** [88.54(13)°][22] and **8** [88.95(5)°] is likely a result of the relatively larger van der Waals radius of Sn (Figure 2 and Table 1).[23] The sum of the bond angles about the square plane defined by the group-14 elements in the N_2O_2 pocket (*i.e.*, $\Sigma\theta_{1-4}$) is less than 360° and decreases with increasing size of the group-14 atom [**8**: 343.77(5)°; **9**: 339.28(14)°[22]; **10**: 332.41(18)°]. Moreover, a larger group-14 atom experiences a greater displacement from the N_4O_2 plane (**8**: 0.467 Å; **9**: 0.593 Å[22]; **10**: 0.739 Å). This structural change affects the degree of coplanarity between the

Table 1. Notable metrics of solid-state structures **8**–**10**, **8**$^{\bullet-}$, and **9**$^{\bullet-}$.

	O2-E-O1 bond angle (θ_1, °)	Sum of angles about E ($\Sigma\theta_{1-4}$, °)	Average dihedral angle (ϕ, °)	Displacement of E from N_4O_2 plane (Å)
8	88.95(5)	343.77(5)	22.4	0.467
9[22]	88.54(13)	339.28(14)	22.6	0.593
10	94.58(18)	332.41(18)	26.8	0.738
8$^{\bullet-}$	86.65(16)	345.90(17)	10.5	0.445
9$^{\bullet-}$	88.07(9)	342.58(10)	13.5	0.531

N-aryl substituents relative to the N_4O_2 plane (Figure 2d and Table 1) and thereby reduces the overlap between the corresponding π systems. We also compared the average dihedral angles [$\phi = (\phi_1 + \phi_2)/2$] between the *N*-aryl substituents and the N_4O_2 plane and found that ϕ was larger for complex **10** (ϕ = 26.81°) than for complexes **8** (ϕ = 22.44°) and **9** (ϕ = 22.63°).[22] The increased deviation from planarity hampers electron delocalization and diminishes the electron-accepting properties of complex **10**, as as evidenced by the CV experiments discussed above.

Upon chemical reduction, the N_2O_2 binding pockets of radicals **8**$^{\bullet-}$ and **9**$^{\bullet-}$ undergo a geometric change. The sums of the bond angles about the group-14 elements in **8**$^{\bullet-}$ and **9**$^{\bullet-}$ become closer to 360° [**8**$^{\bullet-}$: 345.90(17)°; **9**$^{\bullet-}$: 342.58(10)°] compared to **8** [343.77(5)°] and **9** [339.28(14)°][22] and the group-

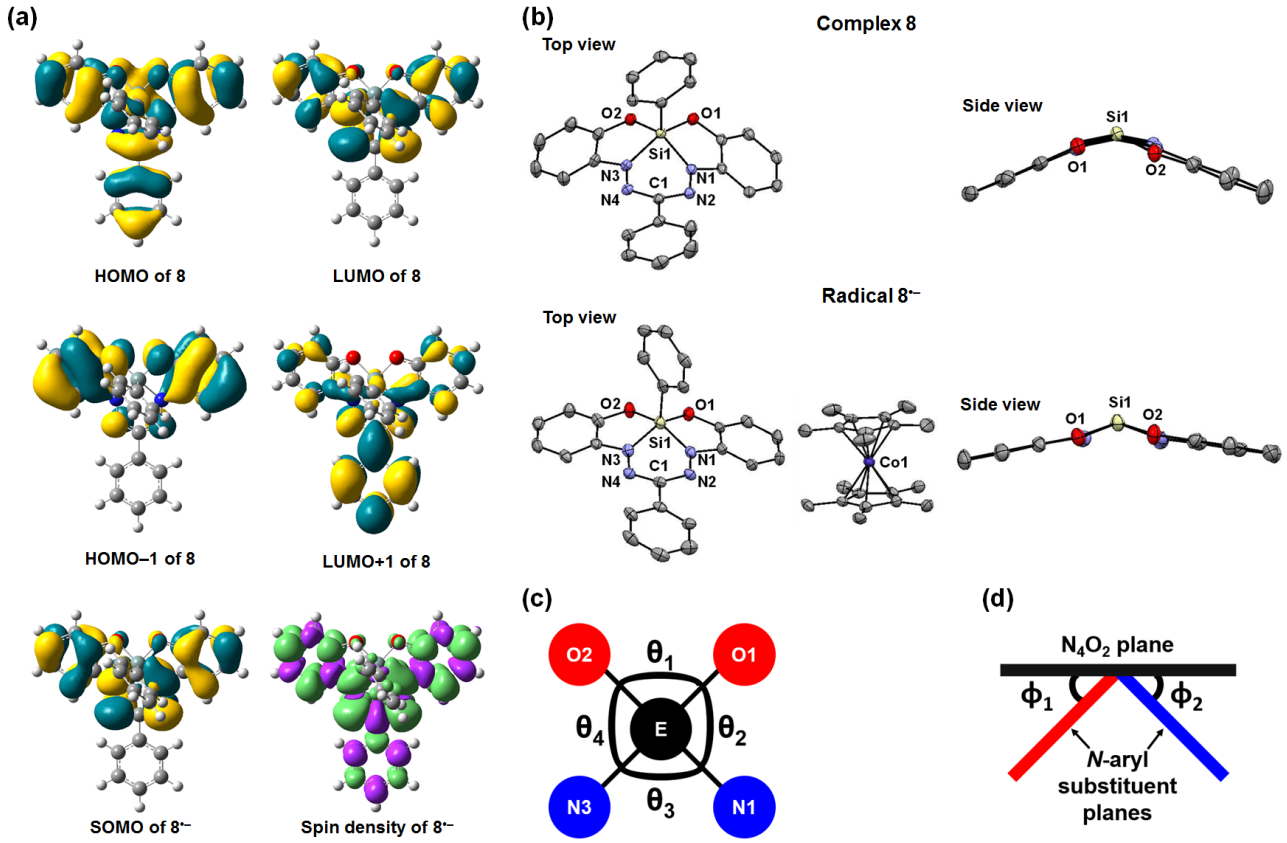

Figure 2. (a) Molecular orbitals of **8** and **8**$^{\bullet-}$ and the spin density of **8**$^{\bullet-}$ calculated at the PBE1PBE/6-311+G* level of theory in CH_2Cl_2 solution. (b) Top and side views of the solid-state structures of **8** and **8**$^{\bullet-}$. Anisotropic displacement ellipsoids are shown at the 50% probability level and the hydrogen atoms and apical-phenyl substituents (side views) have been omitted for clarity. (c) Graphical depiction of the N_2O_2 binding pocket looking at various bond angles θ_{1-4}. (d) The method used to calculate the dihedral angles ϕ_1 and ϕ_2.

14 atoms are drawn closer to the N_4O_2 plane than in the parent complexes (**8**: 0.467 Å vs. **8**$^{\bullet-}$: 0.445 Å and **9**: 0.593 Å[22] vs. **9**$^{\bullet-}$: 0.531 Å). The decrease in ϕ (**8**$^{\bullet-}$: 10.49°; **9**$^{\bullet-}$: 13.52°) is consistent with an increased coplanarity between the *N*-aryl substituents and the N_4O_2 plane. Such structural changes would be disfavored by a larger group-14 atom such as Sn, which would explain the observed instability of radical **10**$^{\bullet-}$.

The average N-N bond lengths in complexes **8–10** are intermediate between typical single and double N-N bonds.[24] Chemical reduction causes these bonds to elongate from 1.3124(16) Å in **8** to 1.362(5) Å in **8**$^{\bullet-}$, consistent with the unpaired electron occupying an orbital with antibonding N-N character (Figure 2a). A similar trend was observed when **9** [1.312(5) Å][22] was reduced to **9**$^{\bullet-}$ [1.357(3) Å]. In addition, chemical reduction results in shorter N-E bonds [**8**: 1.8834(12) Å vs. **8**$^{\bullet-}$: 1.832(4) Å and **9**: 1.986(4) Å vs. **9**$^{\bullet-}$: 1.929(2) Å][22] and longer C-E bonds [**8**: 1.8580(14) Å vs. **8**$^{\bullet-}$: 1.879(5) Å and **9**: 1.922(5) Å[22] vs. **9**$^{\bullet-}$: 1.948(3) Å] of the apical phenyl substituent.

In conclusion, we have prepared and characterized a family of formazanate complexes **8–10** of hypervalent group-14 elements. The electron-accepting properties of these complexes were confirmed using CV; their chemical reduction with $CoCp^*_2$ resulted in stable radicals containing Si (**8**$^{\bullet-}$)and Ge (**9**$^{\bullet-}$). Our inability to isolate an analogous Sn-containing radical was supported by CV experiments, revealing irreversible reduction events at more negative potentials compared to the Si- and Ge-containing species. We rationalized these findings by observing that the π-electron systems of formazanate complexes of Si, Ge, and Sn become less planar as the size of the group-14 atom increases and by linking larger deviations from planarity with a lower stability of the corresponding radical anion. X-ray crystallography and UV-vis absorption spectroscopy suggested that the unpaired electron density in **8**$^{\bullet-}$ and **9**$^{\bullet-}$ was the highest on the formazanate ligand and this was confirmed by EPR spectroscopy. Thus, electron delocalization and stabilitzation by multiple electronegative atoms in complexes **8** and **9** allowed us to isolate group-14-containing radicals in the absence of significant steric bulk.

Acknowledgements:

This work was supported by the Natural Sciences and Engineering Research Council (NSERC) of Canada (J.B.G., DG, RGPIN-2013-435675; V.N.S., DG, RGPIN-2015-04814, R.R.M., CGS-D Scholarship), the Ontario Ministry of Research and Innovation (J.B.G., ERA, ER-14-10-147) and the Canadian Foundation for Innovation (J.B.G., JELF, 33977). The authors thank Dr. Paul Bazylewski and Dr. Giovanni Fanchini for assistance with EPR measurements and access to instrumentation.

Keywords: Stable radicals • Group-14 heterocycles • Redox chemistry • Main-group chemistry • Formazanate ligands

[1] a) P. P. Power, *Chem. Rev.* **2003**, *103*, 789–810; b) P. P. Power, *Nature* **2010**, *463*, 171–177.

[2] a) R. G. Hicks, *Org. Biomol. Chem.* **2007**, *5*, 1321–1338; b) R. G. Hicks, *Stable Radicals: Fundamentals and Applied Aspects of Odd-Electron Compounds*, John Wiley & Sons, Ltd, **2010**.

[3] a) V. Y. Lee, A. Sekiguchi, *Eur. J. Inorg. Chem.* **2005**, 1209–1222; b) V. Y. Lee, A. Sekiguchi, *Acc. Chem. Res.* **2007**, *40*, 410–419.

[4] M. M. Olmstead, L. Pu, R. S. Simons, P. P. Power, *Chem. Commun.* **1997**, 1595–1596.

[5] A. Sekiguchi, T. Matsuno, M. Ichinohe, *J. Am. Chem. Soc.* **2001**, *123*, 12436–12437.

[6] A. Sekiguchi, T. Fukawa, V. Y. Lee, M. Nakamoto, *J. Am. Chem. Soc.* **2003**, *125*, 9250–9251.

[7] A. Sekiguchi, T. Fukawa, M. Nakamoto, V. Y. Lee, M. Ichinohe, *J. Am. Chem. Soc.* **2002**, *124*, 9865–9869.

[8] C. D. Martin, M. Soleilhavoup, G. Bertrand, *Chem. Sci.* **2013**, *4*, 3020–3030.

[9] a) M. Soleilhavoup, G. Bertrand, *Acc. Chem. Res.* **2015**, *48*, 256–266; b) M. Melaimi, R. Jazzar, M. Soleilhavoup, G. Bertrand, *Angew. Chem. Int. Ed.* **2017**, *56*, 10046–10068.

[10] S. Roy, A. C. Stückl, S. Demeshko, B. Dittrich, J. Meyer, B. Maity, D. Koley, B. Schwederski, W. Kaim, H. W. Roesky, *J. Am. Chem. Soc.* **2015**, *137*, 4670–4673.

[11] a) L. Bourget-Merle, M. F. Lappert, J. R. Severn, *Chem. Rev.* **2002**, *102*, 3031–3066; b) C. Camp, J. Arnold, *Dalton Trans.* **2016**, *45*, 14462–14498.

[12] W. D. Woodul, E. Carter, R. Müller, A. F. Richards, A. Stasch, M. Kaupp, D. M. Murphy, M. Driess, C. Jones, *J. Am. Chem. Soc.* **2011**, *133*, 10074-10077.

[13] X. Lu, H. Cheng, Y. Meng, X. Wang, L. Hou, Z. Wang, S. Chen, Y. Wang, G. Tan, A. Li, W. Wang, *Organometallics* **2017**, *36*, 2706–2709.

[14] a) A. W. Nineham, *Chem. Rev.* **1955**, *55*, 355–483; b) G. I. Sigeikin, G. N. Lipunova, I. G. Pervova, *Russ. Chem. Rev.* **2006**, *75*, 885–900.

[15] R. R. Maar, A. Rabiee Kenaree, R. Zhang, Y. Tao, B. D. Katzman, V. N. Staroverov, Z. Ding, J. B. Gilroy, *Inorg. Chem.* **2017**, *56*, 12436–12447.

[16] M. J. Frisch, G. W. Trucks, H. B. Schlegel, G. E. Scuseria, M. A. Robb, J. R. Cheeseman, G. Scalmani, V. Barone, B. Mennucci, G. A. Petersson, H. Nakatsuji, M. Caricato, X. Li, H. P. Hratchian, A. F. Izmaylov, J. Bloino, G. Zheng, J. L. Sonnenberg, M. Hada, M. Ehara, K. Toyota, R. Fukuda, J. Hasegawa, M. Ishida, T. Nakajima, Y. Honda, O. Kitao, H. Nakai, T. Vreven, J. A. Montgomery Jr., J. E. Peralta, F. Ogliaro, M. Bearpark, J. J. Heyd, E. Brothers, K. N. Kudin, V. N. Staroverov, R. Kobayashi, J. Normand, K. Raghavachari, A. Rendell, J. C. Burant, S. S. Iyengar, J. Tomasi, M. Cossi, N. Rega, J. M. Millam, M. Klene, J. E. Knox, J. B. Cross, V. Bakken, C. Adamo, J. Jaramillo, R. Gomperts, R. E. Stratmann, O. Yazyev, A. J. Austin, R. Cammi, C. Pomelli, J. W. Ochterski, R. L. Martin, K. Morokuma, V. G. Zakrzewski, G. A. Voth, P. Salvador, J. J. Dannenberg, S. Dapprich, A. D. Daniels, Ö. Farkas, J. B. Foresman, J. V. Ortiz, J. Cioslowski, D. J. Fox, *Gaussian Development Version*, Revision I.13, Gaussian Inc., Wallingford, CT, 2016.

[17] a) M. Ernzerhof, G. E. Scuseria, *J. Chem. Phys.* **1999**, *110*, 5029–5036; b) C. Adamo, V. Barone, *J. Chem. Phys.* **1999**, *110*, 6158–6170.

[18] a) J. B. Gilroy, M. J. Ferguson, R. McDonald, B. O. Patrick, R. G. Hicks, *Chem. Commun.* **2007**, 126–128; b) M. C. Chang, E. Otten, *Chem. Commun.* **2014**, *50*, 7431–7433; c) M.-C. Chang, T. Dann, D. P. Day, M. Lutz, G. G. Wildgoose, E. Otten, *Angew. Chem. Int. Ed.* **2014**, *53*, 4118–4122; d) M.-C. Chang, A. Chantzis, D. Jacquemin, E. Otten, *Dalton Trans.* **2016**, *45*, 9477–9484; e) S. M. Barbon, V. N. Staroverov, J. B. Gilroy, *Angew. Chem. Int. Ed.* **2017**, *56*, 8173–8177.

[19] S. Stoll, A. Schweiger, *J. Magn. Reson.* **2006**, *178*, 42–55.

[20] a) N. Sakamoto, C. Ikeda, M. Yamamura, T. Nabeshima, *J. Am. Chem. Soc.* **2011**, *133*, 4726–4729; b) M. Yamamura, M. Albrecht, M. Albrecht, Y. Nishimura, T. Arai, T. Nabeshima, *Inorg. Chem.* **2014**, *53*, 1355–1360.

[21] A. W. Addison, T. Nageswara Rao, J. Reedijk, J. van Rijn, G. C. Verschoor, *J. Chem. Soc., Dalton Trans.* **1984**, 1349–1356.

[22] The asymmetric unit for **9** contains two molecules in distinct conformations. Average metrics have been included for simplicity.

[23] M. Mantina, A. C. Chamberlin, R. Valero, C. J. Cramer, D. G. Truhlar, *J. Phys. Chem. A* **2009**, *113*, 5806–5812.

[24] J. R. Rumble, *CRC Handbook of Chemistry and Physics, 98th Edition*, CRC Press/Taylor and Francis, Boca Raton, FL.

Entry for the Table of Contents

COMMUNICATION

Chemical reduction of formazanate complexes of hypervalent group-14 elements results in stable radical anions containing Si and Ge. These radicals are stabilized not by bulky substituents but through electron delocalization over the formazanate ligand, which is enabled by an unusual square-pyramidal coordination geometry of the group-14 atom in the parent complexes.

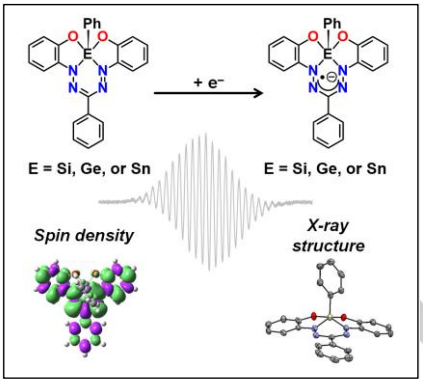

*Ryan R. Maar, Sara D. Catingan, Viktor N. Staroverov, Joe B. Gilroy**

Page No. – Page No.

Formazanate Complexes of Hypervalent Group-14 Elements as Precursors to Electronically Stabilized Radicals